HHS Public Access

Author manuscript

*Prog Neurobiol*. Author manuscript; available in PMC 2024 August 07.

Published in final edited form as:

*Prog Neurobiol*. 2024 August ; 239: 102635. doi:10.1016/j.pneurobio.2024.102635.

# Calcium plays an essential role in early-stage dendrite injury detection and regeneration

**Vinicius N. Duarte**[a], **Vicky T. Lam**[a], **Dario S. Rimicci**[a], **Katherine L. Thompson-Peer**[a,b,c,d,*]

[a]Dept of Developmental and Cell Biology, University of California, Irvine, United States

[b]Center for the Neurobiology of Learning and Memory, Irvine, CA, United States

[c]Sue and Bill Gross Stem Cell Research Center, Irvine, CA, United States

[d]Reeve-Irvine Research Center, Irvine, CA, United States

## Abstract

Dendrites are injured in a variety of clinical conditions such as traumatic brain and spinal cord injuries and stroke. How neurons detect injury directly to their dendrites to initiate a pro-regenerative response has not yet been thoroughly investigated. Calcium plays a critical role in the early stages of axonal injury detection and is also indispensable for regeneration of the severed axon. Here, we report cell and neurite type-specific differences in laser injury-induced elevations of intracellular calcium levels. Using a human KCNJ2 transgene, we demonstrate that hyperpolarizing neurons only at the time of injury dampens dendrite regeneration, suggesting that inhibition of injury-induced membrane depolarization (and thus early calcium influx) plays a role in detecting and responding to dendrite injury. In exploring potential downstream calcium-regulated effectors, we identify L-type voltage-gated calcium channels, inositol triphosphate signaling, and protein kinase D activity as drivers of dendrite regeneration. In conclusion, we demonstrate that dendrite injury-induced calcium elevations play a key role in the regenerative response of dendrites and begin to delineate the molecular mechanisms governing dendrite repair.

### Keywords

Dendrite injury; Dendrite repair; Dendrite regeneration; Drosophila; Calcium; Injury detection

## 1. Introduction

Dendrites are injured during stroke, neurodegenerative disease, traumatic brain injury, and other pathological insults to the CNS (Kiernan et al., 2011; Brown et al., 2007; Mauceri et



*Correspondence to: UC Irvine, Dept of Developmental and Cell Biology, Irvine, CA 92697, United States. ktpeer@uci.edu (K.L. Thompson-Peer).

Declaration of Competing Interest

The authors declare that they have no known competing financial interests or personal relationships that could have appeared to influence the work reported in this paper.

Appendix A. Supporting information

Supplementary data associated with this article can be found in the online version at doi:10.1016/j.pneurobio.2024.102635.

al., 2020; Xiong et al., 2019). While considerable strides have been made in understanding how neurites degenerate (reviewed in (Ding and Hammarlund, 2019; Furusawa and Emoto, 2021) and how axons regenerate (reviewed in (Mahar and Cavalli, 2018; Hao and Collins, 2017) after nervous system insult, the mechanisms under which dendrites detect injury and initiate a regenerative response are not fully understood. Recent discoveries using highly targeted laser injury to dendritic arborization (da) neurons of *Drosophila* have illuminated many processes underlying dendrite regeneration. The dendritic arborization (da) neurons of *Drosophila* are genetically targetable peripheral sensory neurons that are grouped into several classes (I-IV) and pattern the surface of the transparent larval body wall, making them optically accessible (Grueber et al., 2002). This stereotyped anatomy makes them easy to track over multiple days, and they regenerate their dendrites, albeit incompletely, after highly targeted laser injury (Song et al., 2012; Stone et al., 2014; Thompson-Peer et al., 2016). Coupled with the powerful genetic tools available to fly researchers, this model system has allowed us to begin uncovering the molecular mechanisms underlying dendrite regeneration.

Mechanistically, both dendrite and axon repair are sensitive to conserved cell cycle regulators such as the PTEN/PI3K/Akt pathway in flies (Song et al., 2012) and mammals (Park et al., 2008). On the other hand, many lines of evidence suggest that neurons can differentially detect and respond to axon or dendrite injury. For example, axon regeneration requires *DLK-1* (dual leucine zipper kinase-1, also known as *Wallenda* in flies) in both vertebrates and invertebrates, including the da neurons in Drosophila (Stone et al., 2014; Hammarlund et al., 2009; Shin et al., 2012; Xiong et al., 2010; Yan et al., 2009), but *DLK-1/Wallenda* is dispensable for dendrite injury detection and dendrite regeneration in da neurons (Stone et al., 2014). Furthermore, relocalization of the endoplasmic reticulum (ER) to the growing tip only happens during axon regeneration in da neurons, and is not observed during dendrite regeneration (Rao et al., 2016). Kinetochore proteins are necessary for dendrite regeneration, but dispensable for axon regeneration in da neurons (Hertzler et al., 2020). Lastly, the neuronal cytoskeleton responds differentially to dendrite and axon injury, with axon injury resulting in much greater levels of microtubule up-regulation compared to dendrite injury (Stone et al., 2010). Together, these studies provide an explanation for why regenerative mechanisms diverge and suggest that early-stage injury detection could be different for dendrites and axons.

Multiple lines of evidence support the theory that a specific method of dendrite injury detection must exist in neurons. First, in the absence of injury, the dendrites of class I da neurons are mostly stable in number, developing a negligible number of branches over late larval development. After complete dendrite removal, however, class I neurons do initiate new branch formation and fully regenerate their original branch number (Stone et al., 2014; Thompson-Peer et al., 2016). Second, in adult *Drosophila*, class IV neurons maintain constant dendrite length over a week of adulthood, but dendrite removal triggers these neurons to significantly recover dendrite length (DeVault et al., 2018). Lastly, dendrite injury induces changes in gene expression that have regenerative consequences for injured neurons (Hertzler et al., 2020). These studies together suggest that dendrite regeneration is a phenomenon that is separable from dendrite development and dendrite dynamics; one that is likely triggered by some injury detection mechanism.

Before repair can begin, neurons must first sense that they have been injured. Axonal crush injury has been shown to induce global membrane depolarization in neurons of the buccal ganglion of the mollusc (Strautman et al., 1990), and elevation of intracellular calcium levels have been observed after axonal transection to *ex-vivo* lamprey spinal axons and cultured Aplysia neurons (Berdan et al., 1993; Ziv and Spira, 1993, 1995). *In-vivo* studies in *C. elegans* motor neurons support that this injury-induced rise in intracellular calcium is necessary for axon regeneration, and further showed that it correlates to regenerated length of the axon and is sufficient to drive enhanced repair (Ghosh-Roy et al., 2010). Axon injury to dorsal root ganglia (DRG) neurons of mice also triggers elevations in calcium, which activate PKC$\mu$ (protein kinase C $\mu$; PKD in flies) and subsequently drives axonal repair (Cho et al., 2013). While these studies provide great insights into our understanding of how neurons use calcium to detect and respond to axon injury, the extent to which calcium contributes to *dendrite* injury detection and repair remains unknown.

Here, we use the *Drosophila* da neuron model system and 2-photon laser injury to investigate whether early calcium influx after dendrite injury promotes dendrite repair and how calcium channels and effectors influence regeneration. Our results demonstrate that dendrite injury triggers global calcium influx into the cytosol. We observed that dendrite or axon injury to the same cell type triggers varying degrees of intracellular calcium elevations. Furthermore, we observe impaired calcium influx in chronically hyperpolarized neurons and impaired dendrite regeneration in these neurons hyperpolarized only at the time of injury. Lastly, RNAi-mediated knockdown of L-type voltage-gated calcium channels (VGCCs), perturbations of $IP_3$ signaling, and inhibition of Protein Kinase D activity all dampen dendrite regeneration. Altogether, these data suggest that early calcium elevations help drive dendrite regeneration and provide novel mechanistic insights into dendrite injury detection and repair.

## 2. Results

### 2.1. Dendrite injury triggers rapid somatic calcium influx

To examine the extent of calcium influx following neurite injury, we used a 2-photon laser to sever either a dendrite or an axon of larval da neurons expressing the genetically encoded calcium indicator GCaMP7f (Dana et al., 2019). 2-photon laser injuries were conducted at 72 h after egg lay (AEL), and neurites were injured ~30–50μm away from the cell body. We chose this distance because axon severing closer to the cell body often fails to initiate a regenerative program directly from the injured stump (Stone et al., 2010) and so that we could effectively measure the temporal dynamics of calcium wave backpropagation after injury to either neurite. Somatic calcium levels were continuously imaged for ~3 minutes in live, intact animals, with injuries occurring approximately 7.25 seconds after the start of the imaging session. Following live imaging, larvae were individually housed, then imaged ~24 h after injury to confirm neuronal survival and neurite severing. To quantify the extent of calcium influx after targeted laser injury, we measured the somatic $\Delta F/F_0$ (see methods for calculation) for each movie and plotted the $\Delta F/F_0$ calcium trace, peak $\Delta F/F_0$, and time to peak $\Delta F/F_0$. A timeline of calcium imaging and regeneration assays used throughout the study are provided in Fig. 1A; graphics of neurons used in this study are depicted in Fig. 1B.

We first severed either a dendrite or an axon of the dorsal class I neuron ddaE from abdominal segment 2, 3, 4, or 5. We measured early calcium influx at the soma, as this is where GCaMP signals accumulate. Axon injury to these da neurons triggered rapid global calcium influx (Fig. 1C), which is in agreement with experiments in *C. elegans* and mammalian cell culture (Ghosh-Roy et al., 2010; Wolf et al., 2001). We found that dendrite injury also triggers a rapid global calcium influx (Fig. 1C). Quantification and plotting of the somatic $\Delta F/F_0$ calcium traces show that dendrite and axon injuries produce similar injury-induced calcium influx in class I da neurons (Fig. 1D), with similar average peak somatic $\Delta F/F_0$ (Fig. 1E) and similar average time to peak $\Delta F/F_0$ (Fig. 1F). The variance of peak somatic $\Delta F/F_0$, however, was significantly greater after dendrite injury (Fig. 1E, F-test = 7.0, $p = 0.0022$), likely due to differences in dendritic architecture among injured neurons of the same type (class I da neurons), whereas injured axons share near identical morphology. These data suggest that dendrite injury induces rapid elevations in intracellular calcium that are temporally similar to axon injury-induced calcium influx.

Both class I and class IV da neurons regenerate dendrite branches after injury (Song et al., 2012; Thompson-Peer et al., 2016). However, class I ddaE neurons exhibit inconsistent axon regeneration from the injured axon stump, while class IV ddaC neurons more reliably regenerate an axon from an injured stump (Rao and Rolls, 2017; Song, 2012). These ddaC neurons also exhibit greater morphological complexity (Grueber et al., 2002), continuously add branches throughout larval development, and serve different sensory functions for the organism (Hughes and Thomas, 2007; Parrish et al., 2009; Xiang, 2010). To determine whether class IV da neurons exhibit any differences in injury-induced calcium influx, we severed either a dendrite or an axon of the dorsal class IV neuron ddaC, again from abdominal segments 2, 3, 4, or 5. In ddaC neurons, we observed that both axon and dendrite injury triggers an increase in somatic calcium levels, but to different extents (Fig. 1G). Axon injury induces significantly higher and faster somatic calcium influx than dendrite injury (Fig. 1H), with a higher average peak somatic $\Delta F/F_0$ (Fig. 1I) and a faster average time to peak somatic $\Delta F/F_0$ for axon injury than dendrite injury (Fig. 1J). Compared to class I ddaE neurons, these high levels of calcium influx after axon injury to class IV ddaC neurons may explain why they exhibit more consistent stump regeneration.

Class IV da neurons are responsive to blue and UV light stimulation (Xiang et al., 2010) so we performed control experiments in which the bleaching laser power was set to 0.02 %, a power insufficient to produce injury, and imaged GCaMP levels as described in the methods. Laser-scanning alone did not change somatic calcium levels in class I or class IV da neurons (Supplemental Figure 1 A).

To determine whether injury-induced calcium influx has a regenerative consequence, we simultaneously measured initial calcium entry and the resulting branch repair in two types of class I neurons (dorsal ddaE and ventral vpda neurons) via co-expression of GCaMP7f and a membrane-bound tdTomato fluorophore. GCaMP7 levels were imaged during distal primary branch injuries, branch severing was confirmed 24 hours later, and regenerative branch addition was assessed at 72 hours post-injury (PI). Neither ddaE nor vpda neurons showed correlations between peak somatic $\Delta F/F_0$ and the number of regenerated branches (Supp Figs. 1B and 1 C). These data suggest that injury-induced calcium influx may exhibit

cell type and neurite specificity. Unlike axons, dendrite injury-induced calcium influx does not correlate with the extent of dendrite regrowth.

In experimenting with class I vpda neurons, we occasionally observed that the GCaMP signal would decrease as normal in the cytosol but persist in the nucleus (we refer to this as cytosolic GCaMP clearance). This was observed in 58.33 % of neurons tested (7/12). Representative images of class vpda neurons with and without cytosolic GCaMP clearance are shown in Supp Fig. 1D. To the best of our knowledge, cytosolic GCaMP clearance, or nuclear GCaMP persistence, has never been described in the context of injury. One study has described aberrant nuclear GCaMP accumulation in the context of excitation-transcription coupling in cortical neurons *in vitro* (Yang et al., 2018). Nonetheless, our data suggest that this observation did not affect regenerative outcomes.

### 2.2. Injury-induced calcium influx is not sensitive to distance in class I ddaE neurons, but it is in class IV ddaC neurons

Electrophysiological recordings in the buccal ganglion of the mollusk have shown that somatic membrane depolarization is substantially reduced in a distance-dependent manner after axon injury (Berdan et al., 1993). Given this, we sought to determine whether the site of dendrite injury affects injury-induced calcium influx. To determine how dendrite injury at different sites along a dendrite arbor would affect calcium influx, we injured either a terminal or proximal branch of class I ddaE neurons along the comb dendrite and measured somatic calcium influx (Figs. 2A and 2B). Despite significantly different injury distances between groups (Supp Fig. 2A), we were surprised to find that different injury distance resulted in similar somatic calcium influx in these neurons (Fig. 2C–E). In class IV ddaC neurons, however, we did in fact observe an injury distance-dependent effect on somatic calcium influx (Fig. 2F).

Previous studies suggest that the presence of a dendrite stump 24 h after injury is deterministic of whether a class IV neuron will regenerate from the site of injury (Song et al., 2012). Therefore, we chose to injure class IV ddaC neurons right next to the cell body leaving no stump (proximal “no stump” group), slightly farther away from the cell body along a primary branch (“stump” group), or far from the cell body (“distal”) (Fig. 2E), which are injury distances significantly different from one another (Supp Fig. 2B). Distal injuries produced dramatically lower $\Delta F/F_0$ compared to no stump and stump groups (Fig. 2H), resulting in lower peak $\Delta F/F_0$ (Fig. 2I) and longer time to $\Delta F/F_0$ (Fig. 2J). Thus, injury-induced somatic calcium influx is sensitive to distance in class IV but not class I neurons. Together, this suggests that different neuronal cell types have varying capacities for calcium-mediated dendrite injury detection, with some neurons being highly responsive to injuries anywhere along their arbor (class I) while others may have an impaired ability to detect dendrite injury at more distal regions (class IV).

### 2.3. Dendrite injury at different sites triggers varying levels of dendrite regeneration

Regenerative outcomes of both class I and class IV da neuron axons have been shown to differ as a function of distance from the cell body (Rao and Rolls, 2017). Axon injury near the soma resulted in more instances of dendrite-to-axon conversion while distal injuries

resulted in more instances of regeneration from the injured axon stump, observations noted in both class I and class IV neurons (Rao and Rolls, 2017). To determine whether injury distance influences regenerative outcomes for these neurons, we chose to sever them at varying distances from the cell body as in Figs. 2A and 2E.

For class I neurons, we measured regeneration by normalizing for the number of branches lost. In other words, if a neuron had 5 branches removed, regeneration was measured by branch number (BN) at 72 h PI – (BN before injury – 5). Regenerative outcomes after a single branch injury to ddaE neurons are typically observed as short branches being added to the spared dendrite arbor. We refer to this as “regeneration”, not “sprouting”, based on terminology used in the field of axon regeneration (Tuszynski and Steward, 2012). As the primer outlines, the term sprouting is reserved for compensatory growth of uninjured axons after injury to neighboring axons. In contrast, regrowth observed from the injured axon but at a location distinct from the site of injury, as we see here with our ddaE dendrites, is still referred to as regeneration. We keep this framework in mind for these experiments and for subsequent experiments utilizing single branch injuries to class I ddaE neurons. Neurons regrew significantly more dendrite branches after proximal injury compared to terminal branch injury (Figs. 3A and 3B). Moreover, the location of growth was different: proximal injuries also triggered more instances of regenerative growth from the site of injury (6/14 neurons or 43 %) while terminal branch injuries never triggered regrowth from the site of injury (Fig. 3D). These data suggest that the amount of dendrite regeneration in class I ddaE neurons depend on the proximity of injury, or the number of branches removed. Further, injury proximity may confer a neuron with the ability to regenerate from the injured stump.

Class IV ddaC neurons typically extend longer primary branches than class I ddaE neurons, so they served as an excellent model for testing whether a spared stump would facilitate regeneration from the injury site. As for Fig. 2f–j, we again injured next to the cell body (“no stump”), near to the cell body (“stump”), or far from the cell body (“distal”). After each of these injuries, we observed growth of new dendrite branches. In the no stump group, 11/13 (85 %) neurons completely failed to regenerate from the site of injury (Figs. 3D and 3E). The two neurons that were included in the “Yes” group completely remodeled their dendritic arbors after injury to only one branch, but indeed regenerated from the injury site. For both the stump and distal groups, over 70 % of neurons regenerated from the site of injury (Figs. 3D and 3E). Previous data has suggested that reversal of dendritic microtubule polarity (retrograde to anterograde, or minus-end out to plus-end out) is necessary for regeneration from the site of injury (Song et al., 2012). Given our data, the sparing of a dendritic stump after injury may facilitate this microtubule polarity reversal in the injured stump.

### 2.4. Hyperpolarized neurons experience shunted injury-induced calcium influx

Several studies in both mammalian and invertebrate systems have used a human KCNJ2/KiR2.1 transgene to determine how electrical activity affects neuronal repair. Each of these studies concluded that electrical activity supports neurite repair, as evidenced by suppressed axon (Li et al., 2016; Wang et al., 2023) or dendrite (Thompson-Peer et al., 2016) regeneration in neurons expressing the transgene. The original paper that first cloned

this transgene showed that it inhibits neuronal activity by hyperpolarizing the membrane to about −85 mV in aCC motoneurons of the Drosophila embryonic CNS (Baines et al., 2001). Previous work in the field of calcium-mediated axon injury detection suggested that axon injury triggers membrane depolarization, which is essential for injury-induced calcium influx (Wolf et al., 2001; Mandolesi et al., 2004). Given this, we hypothesized that expressing KCNJ2 in neurons might cause diminished regeneration due to inhibition of injury-induced calcium influx.

To test this hypothesis, we expressed a human KCNJ2/KiR2.1 transgene in class I and class IV neurons and assessed dendrite injury-induced calcium influx and dendrite regeneration. The original KCNJ2 transgene widely used in previous studies contains a GFP-tag, so we opted to use an HA-tagged KCNJ2 transgene. Prior to injury, we observed an elevation of the baseline GCaMP7f signal in class I ddaE neurons expressing this KCNJ2.HA transgene (Supp Fig. 4A). Like the experiments in Fig. 1, we opted to injure dendrites further from the cell body for two reasons: to allow for the backpropagation of a calcium wave, and because this is the observed standard in measuring injury-induced calcium responses after axotomy (Ghosh-Roy et al., 2010; Cho et al., 2013). In class I ddaE neurons, injury-induced somatic $\Delta F/F_0$ values were drastically lower in KCNJ2.HA-expressing neurons compared to controls (Figs. 4A and 4B), and peak somatic $\Delta F/F_0$ were significantly lower in KCNJ.HA-expressing neurons (Fig. 4C). To determine whether this injury method also resulted in a reduction in dendrite branch regeneration, we assessed regeneration in neurons expressing KCNJ2.HA using a distal primary branch injury (Fig. 4D–E). Like our proximal injuries from Fig. 3A, this injury also results in regeneration of small branches, but injured neurons typically over add branches compared to uninjured controls. Dendrite injury results in regeneration, and in fact in branch over-addition compared to uninjured controls. We confirmed that we delivered the same type of dendrite injuries to both wild-type and KCNJ2.HA-expressing neurons (the number of branches removed, length of dendrites removed, and injury distance were not different between groups (Supp Fig. 4 C–E). After injury, we found that KCNJ.HA-expressing neurons regenerated significantly less branches than their wild-type counterparts, and branch addition was indistinguishable from their uninjured counterparts (Fig. 4E). We also assessed injury-induced calcium influx in class IV ddaC neurons expressing KCNJ2.HA and found that these neurons also experience shunted injury-induced calcium influx (Fig. 4H–J). Together, these data suggest that KCNJ2 inhibits regeneration in part via the shunting of injury-induced calcium influx.

Since KCNJ2 expression was also shown to impair axon regeneration (Li et al., 2016; Wang et al., 2023), we also conducted calcium imaging experiments after axon injury. Peak somatic $\Delta F/F_0$ was also significantly reduced after axon injury in class I ddaE neurons expressing the KCNJ2. HA transgene (Supp Fig. 4B). Since this KCNJ2.HA-tagged transgene is a newer transgenic tool to hyperpolarize the neuron, we also sought to reproduce previous findings that fully balded class I or class IV neurons expressing KCNJ2.GFP regenerated less than wild-type counterparts (Thompson-Peer et al., 2016). These are experiments where we severed all the dendrite branches, not just one. Our results after balding KCNJ2. HA neurons were congruent with evidence published using the KCNJ2. GFP transgene: both class I and class IV neurons expressing KCNJ2.HA regenerated less well than their wild-type counterparts after balding injury (Supp Fig. 4 F–J).

We also conducted calcium imaging experiments using the traditional GFP-tagged KCNJ2, which has been previously shown to inhibit regeneration in these neurons and found that KCNJ2.GFP also reduced injury-induced somatic calcium influx (Supp Fig. 4 K–M).

While our data provide a mechanism for why KCNJ2-expressing neurons regenerate less well, the constitutive expression does not allow us to rule out the possibility that KCNJ2 expression either during development or during the regenerative period may be impairing regeneration. Thus, we next sought to control KCNJ2 expression in a temporal manner using a temperature-sensitive $Gal80^{ts}$ (McGuire et al., 2003).

### 2.5. Temporal expression of KCNJ2/KiR2.1 at the time of injury blocks dendrite regeneration

To determine whether KCNJ2.HA expression only at the time of injury is sufficient to impair regeneration, we temporally expressed the transgene using the temperature-sensitive Gal80 repressor ($Gal80^{ts}$) in class IV neurons. We chose to return to the KCNJ2.GFP transgene as it does not present a confound for these experiments and because it is the most widely-published KCNJ2 transgene, with 257 citations, compared to the new KCNJ2.HA transgene. At a permissive temperature of 18°C, $Gal80^{ts}$ binds the UAS upstream of the KCNJ2 transgene, thereby preventing binding of Gal4 so that KCNJ2/KiR2.1 will not be expressed in class IV neurons. At a restrictive temperature of 29.5°C, the $Gal80^{ts}$ is unable to bind to UAS, allowing for binding of Gal4 and KCNJ2/KiR2.1 expression. Since temperature affects the rate of larval development, we adjusted the injury timepoint so that animals would be roughly comparable in developmental stage to prior experiments (early third instar; Fig. 5A). We chose to perform these experiments only in class IV neurons because we had a CD4-tdGFP fluorescent marker fused directly downstream of the class IV-specific ppk promoter (ppk-CD4-tdGFP). This direct fusion is critical as $Gal80^{ts}$ would suppress a fluorescent marker downstream of a UAS sequence (UAS-CD4-tdTom as in class I ddaE neurons) upon transfer of organisms to an 18 C incubator. At the time, we were unaware of constructs with a fluorescent marker fused directly downstream of a class I promoter.

In uninjured neurons, we found that temporally inducing expression of the KCNJ2.GFP transgene did not alter dendrite arbor size at 192 h AEL (the timepoint corresponding to 96 h PI; Figs. 5B and 5C). We did observe some morphological differences in uninjured neurons such as blebbing of some distal dendrites and elongated terminal branches, both of which are characteristic of Kir2.1 expression in class IV da neurons. These phenotypes, however, were not as drastic as those seen in neurons with constitutive expression of Kir2.1. This gave us confidence that KCNJ2 was transiently expressed. In injured neurons, we found that wild-type injured neurons regenerated significantly more than injured neurons expressing KCNJ2.GFP only around the time of injury (Fig. 5B, C). Neither genotype was able to regenerate a large enough dendrite arbor to cover the same size as uninjured controls, which is supported by previous findings in wild-type neurons (Thompson-Peer et al., 2016). This data confirms our hypothesis that KCNJ2 expression only at the time of injury is sufficient to inhibit repair, likely due to diminished injury-induced calcium influx.

### 2.6. Dendrite regeneration is sensitive to L-type VGCCs and intracellular $IP_3$ signaling

L-type voltage-gated calcium channels (VGCCs), also known as $CaV_{1.2}$, have been established as mediators of extracellular calcium entry and axonal regrowth after axon injury in NT2 cells, superior cervical ganglion neurons, and in *C. elegans* PLM neurons (Ghosh-Roy et al., 2010; Wolf et al., 2001; Kulbatski et al., 2004). Additionally, these channels regulate dendrite morphogenesis in the PVD neurons of *C. elegans* (Tao et al., 2022). To determine whether L-type VGCCs are involved in dendrite injury-induced calcium and repair in our da neurons, we knocked down transcripts of the Ca-α1D gene using RNAi. This gene codes for the main pore-forming subunit of L-type VGCCs. To avoid the developmental confounds associated with branch dynamics during larval development in class IV neurons, these experiments were conducted solely in class I ddaE neurons that establish and maintain branch number throughout larval development (Stone et al., 2014). In uninjured neurons, expression of this RNAi did not change total branch number nor total dendrite length at 144 h AEL (Supp Figs. 6A and 6B). In injured neurons, we found that RNAi expression resulted in significantly less branch regrowth after injury (Figs. 6A and 6B). We confirmed that there were no differences in the type of injury delivered to wild-type versus RNAi neurons, by measuring number of reduced branches, length of dendrites removed, and injury distance (Supp Fig. 6 C–E). We did not observe any differences in peak somatic $\Delta F/F_0$ (Supp Fig. 6 F–G). Taken together, these data suggest that L-type VGCCs may be mediators of dendritic regrowth after dendrite injury, but they alone are not responsible for injury-induced calcium influx.

In addition to calcium entry from outside the cell, intracellular, ER-bound calcium release channels (namely $IP_3$ receptors and ryanodine receptors) are involved in intracellular calcium elevations after axon injury (Wolf et al., 2001) and promote axon repair *in vivo* (Ghosh-Roy et al., 2010; Sun et al., 2014). Studies examining stimulation-induced calcium release in hippocampal neurons have noted that these calcium release channels are localized to dendritic branch points (Fitzpatrick et al., 2009), suggesting a possible role in dendrite morphogenesis or dendrite regeneration. To test whether the $IP_3$ signaling affects dendrite regeneration, we expressed a dominant-negative $IP_3$ sponge transgene in class I ddaE neurons (Usui-Aoki et al., 2005). In uninjured neurons, we observed no differences in total branch number nor total dendrite length at 144 h AEL (Supp Figs. 6 H and 6I). In injured neurons, we observed a significant decrease in dendrite branch regrowth for neurons expressing the $IP_3$ sponge (Figs. 6C and 6D). For this dataset, the number of branch and total dendrite length removed were no different between groups (Supp Figs. 6 J and 6 K). However, IP3 sponge neurons were injured slightly further from the cell body compared to wild-type neurons (Supp Fig. 6 L). While we showed that injury distance has regenerative consequences, those experiments used either proximal or terminal branch injuries, each of which are drastically different from one another (Supp Fig. 2A). Thus, we believe that the difference in injury distance for this dataset did not play a significant role in regenerative outcomes. Lastly, we found no differences in injury-induced somatic calcium influx nor peak somatic calcium influx with this transgene. This was an interesting finding because previous studies using this same $IP_3$ sponge in PLM neurons of *C. elegans* did report reduced GCaMP transients in the severed axons of sponge-expressing neurons (Ghosh-Roy et al., 2010).

### 2.7. PKD activity regulates dendrite regeneration

Drosophila have a single protein kinase D (PKD) gene with high sequence similarity to the three human PKD isoforms PKD1/PKCμ, PKD2, PKD3/PKC*ν*. Maier et al., (2006). In murine hippocampal culture, protein kinase C mu (PKCμ) has been shown to associate with the Golgi-apparatus to regulate neuronal polarity and the trafficking of dendritic membrane proteins (Czöndör et al., 2009; Yin et al., 2008). Further, a RhoA-Rho kinase signaling pathway regulates the formation of polarized Golgi outposts in dendrites of cultured hippocampal neurons and Golgi outposts have been shown to regulate dendritic arborization in da neurons (Quassollo et al., 2015; Ori-McKenney et al., 2012; Zhou et al., 2014). In mouse DRG neurons, axon injury triggers calcium-dependent PKCμ activation that is essential for axonal repair (Cho et al., 2013; Cho and Cavalli, 2012). Given both the developmental and regenerative roles for PKD in nerve cells, we posited that PKD may be involved in dendrite repair.

To test this, we first expressed a dominant-negative PKD transgene (PKD.DN) in class I ddaE neurons and assessed regeneration using our distal primary branch injury assay. In uninjured neurons, we found no differences in total branch number nor total dendrite length at 144 h AEL (Supp Figs. 7D and 7E), nor did we observe any differences in branch addition from 72 h AEL to 144 h AEL (Fig. 7B, uninjured neurons). In injured neurons, expression of the PKD.DN transgene resulted in significantly less branch regrowth (Figs. 7A and 7B). In these experiments, we controlled for the number of branches removed (4–7) and this, along with injury distance, was not different between groups (Supp Figs. 7A and 7 C). However, total length removed was significantly lower in neurons expressing PKD.DN (Supp Fig. 7B). Together, these data implicate PKD in dendrite regeneration but whether this is mechanistically occurring via impaired Golgi outpost formation as in cultured hippocampal neurons or via injury sensing as in axotomized DRG neurons remains unknown.

Because PKD has distinct localization patterns during development or nerve injury, we sought to determine whether dendrite or axon injury to class I ddaE neurons triggers changes in PKD localization. To do this, we expressed a GFP-tagged wild-type version of PKD and injured either a dendrite or an axon of ddaE neurons. After injury to either neurite type, we were unable to observe cytoplasmic to nuclear translocation of PKD. Following dendrite injury, we occasionally observed the formation of PKD puncta either near the nuclear compartment, or at sites along the dendrite arbor (Supplemental Figure 7 G; green arrowheads). It is important to note that these observations were not consistent, but they do suggest a possible role for dendrite injury-induced changes in PKD localization and warrant further investigation into the mechanisms by which PKD affects dendrite repair. We also assessed regeneration with this transgene as we are overexpressing levels of PKD. In these experiments, we found no differences between neurons expressing this transgene in both the uninjured or injured condition (Supp Fig. 7I).

Lastly, we wanted to determine how the constitutively active PKD transgene (PKD.CA) would affect dendrite regeneration. In uninjured neurons of the distal cut regeneration assay, expression of this transgene did not change branch addition (Supp Fig. 7 J). Injured neurons expressing PKD.CA were unable to add significantly more branches than their uninjured

counterparts, but they did add a statistically comparable number of branches as wild-type neurons (Supp Fig. 7 J). In uninjured neurons of the full balding assay, total branch number was not significantly different (Supp Fig. 7 K). In injured neurons, expression of PKD. CA impaired recovery of branch number relative to uninjured controls, an established phenotype for this assay in wild-type neurons (Supp Fig. 7 K). Together, these data suggest that constitutive expression of hyperactive PKD is also inhibitory to regeneration.

## 3. Discussion

Our work provides the first lines of evidence that dendrite injury triggers elevations in calcium influx and that this influx is supportive of dendrite regeneration. In both class I and class IV neurons that are chronically hyperpolarized by the expression of KCNJ2, we observed impaired calcium influx. Previous works have used this transgene to electrically silence neurons and determine whether neuronal activity supports neurite repair. Our data provides a mechanism by which this transgene may be shunting dendrite regeneration. Importantly, temporal expression of KCNJ2 only around the time of injury was sufficient to impair dendrite regeneration, suggesting that preventing neuronal depolarization during and not after injury has consequences for dendrite regeneration. Additionally, we find that dendrite regeneration is sensitive to levels of L-type VGCCs, $IP_3$ signaling and PKD activity. Together, our work demonstrates that calcium increases after injury have morphological consequences for dendrite regeneration.

### 3.1. Injury-induced calcium elevations after neurite injury

Previous studies have quantified axon injury-induced calcium influx at or near the site of injury (Ghosh-Roy et al., 2010), but axotomy-induced calcium waves are thought to travel back to the cell body in order to initiate a regenerative response (Mahar and Cavalli, 2018; Rishal and Fainzilber, 2014). Because of this, we chose quantify axotomy-induced and dendrotomy-induced calcium levels at the cell body, where the initiation of a pro-regenerative transcriptional response is suggested to be induced by elevated calcium levels (Mahar and Cavalli, 2018). We found that calcium levels rise much higher in class IV neurons than in class I neurons after distal axon injury, suggesting that different neuronal types may detect axon injury better than others. This notion is supported by studies showing that distal injuries to class I axons yield less consistent regeneration from the injured stump, while the same distal injury to class IV da neuron axons results in more consistent regrowth from the site of injury (Rao and Rolls, 2017). Furthermore, axotomy-induced calcium influx drives the formation of a regenerative axon growth cone in cultured Aplysia neurons and is deterministic of whether an axon will regenerate (Kamber et al., 2009), supporting our idea that class IV axons may exhibit regenerative resilience attributable to injury-induced calcium influx in comparison with class I neurons.

Dendrites differ from axons in their highly branched morphology, which may change how an injury signal is detected at the cell body. The 2-photon laser injury assay allows us to distinguish the neuronal response to injury of various degrees of severity: severing more or fewer branches, closer to or farther from the cell body, and with more or fewer branch points between the site of injury and the soma. Injury at any distance from the cell body or to

either cell type triggered elevation in intracellular calcium levels that was not confined to the injured neurite or the cell body. This is reminiscent of the observation that axon injury triggers global calcium influx (Wolf et al., 2001). With respect to dendrotomy-induced calcium influx in class I ddaE neurons, dendrite injury to a proximal branch near the cell body resulted in calcium influx with indistinguishable spatiotemporal kinetics as dendrite injury to a terminal branch. This was in stark contrast to class IV ddaC neurons that exhibited reduced levels of calcium influx in a distance-dependent manner. We speculate that the differences in injury-induced calcium influx between class I and class IV neurons may be due to unique biophysical properties of the dendrites or varying distribution of calcium channels along the arbor, which may influence the backpropagation of this injury signal back to the soma. In future studies, it may be of interest to incorporate newly generated, ER-localized calcium indicators such a G-CatchER$^{+}$ (Reddish et al., 2021) to examine how internal calcium stores deplete upon injury and replenish throughout the regenerative process.

### 3.2. Distinguishing between injury types and their respective regenerative responses

One seeming quandary is how neurons differentiate between axon injury and dendrite injury if both can cause similar increases in somatic calcium levels, as is the case in class I ddaE neurons. Axon injury does not cause dendrite branch addition, aside from cases where a dendrite is being converted into an axon (Rao and Rolls, 2017). However, axons also require the activity of the dual leucine zipper kinase DLK-1/Wallenda to detect axon injury, while dendrite injury does not activate DLK-1/Wallenda and dendrite regeneration can occur independent of DLK-1/Wallenda (Stone et al., 2014). Perhaps severe and prolonged injury-induced calcium rises cause dendrite regeneration, while the same calcium rises in conjunction with DLK-1/Wallenda activity cause axon regeneration. Another possibility is that there could be a calcium-regulated protein that is critical and specific to dendrite regeneration. Cytoskeletal disruption has been posited to activate the axon injury sensing DLK/JNK pathway and drive axon regeneration of mammalian neurons (Valakh et al., 2015). This must be a phenomenon specific to axons because dendrite injury also triggers cytoskeletal disruption that does not result in activation of the JNK pathway (Stone et al., 2014). Interestingly, expression of dominant-negative JNK protein in the class I ddaE neuron can change dendritic microtubule polarity, but this only happens for the lateral dendrite that converts into an axon following proximal axotomy. This suggests that JNK signaling plays a role in dendritic microtubule polarity, and that this axon injury-sensing pathway could potentially intersect with dendrite injury-sensing.

Although injury detection gives rise to neurite-specific regrowth, crosstalk between the axonal compartment and the dendrite compartment, and vice versa, after injury, remains likely. Axon injury is known to cause simplification of the dendrite arbor in these class IV neurons, as well as neurons in other systems (Chen et al., 2012). How dendrite injury-induced calcium elevations drive dendrite regeneration while axon injury-induced calcium elevations drive dendrite stabilization (i.e. removal) remains unknown. Indeed, there is evidence that dendrite arbor stabilization after axon injury may be required for axon regeneration (Beckers and Moons, 2019). Whether dendrite regeneration requires

morphological or functional changes in the axonal compartment is an interesting question for future research.

Our distance-dependent regeneration data in class I versus class IV neurons (Fig. 3) yielded perplexing results. In both of these cell types, microtubule orientation has been described as primarily plus-end-out in axonal compartments, minus-end-out in proximal dendritic compartments, and mixed in distal dendrites (Ori-McKenney et al., 2012; Rolls, 2007; Stone et al., 2008). In class IV neurons, convincing evidence has been generated suggesting that regenerative growth from an injured stump relies on microtubule polarity reversal in that stump. If no regrowth occurs from the site of injury, microtubule polarity reversal is observed in a neighboring branch whose dendrite arbor invades the enervated territory (Song et al., 2012). Our data in class IV neurons suggests that injuries very close to the cell body (leaving no stump) result in virtually no instances of regrowth from the site of injury. Conversely, injuries close to the cell body that spare a stump dramatically facilitates regrowth from the injury site. Strikingly, however, the opposite is true for class I neurons. Terminal branch injuries resulted in zero instances of regrowth from the site of injury, while neurons who received a proximal injury regrew dendrites from the injury site about half the time. Regarding injury-induced microtubule dynamics in class I neurons, global-upregulation of microtubule dynamics has been observed after axon injury but this is not evident after proximal dendrite injury (Stone et al., 2010). The role of microtubule dynamics and polarity reversal in these seemingly opposite responses to injury in class I and class IV neurons is an interesting area of future research.

### 3.3. Manipulating electrical activity to study neural repair

Prior studies investigated whether electrical activity is either necessary for or contributes to neuronal regeneration. Several lines of evidence suggest that electrical activity reduces both developmental axon growth and regenerative axon growth due to the competing functions of synaptic transmission and axonal extension (Cohan and Kater, 1986; Enes et al., 2010). On the other hand, the application of functional electrical stimulation (FES) as a therapeutic for neuromuscular disorders and FES's preclinical, pro-regenerative data suggest that stimulating neurons may enhance regeneration (Gordon, 2016; Jara et al., 2020; Javeed et al., 2021; ElAbd et al., 2022). In Drosophila da neurons, chronic inhibition of electrical activity blocks both dendrite and axon regeneration (Thompson-Peer et al., 2016; Wang et al., 2023). When we consider, however, that injury-induced depolarization is necessary for calcium entry to occur and that calcium entry has been tightly linked to regenerative outcomes, this presents a confound. Inhibition of electrical activity must be controlled in a temporal manner and its applications should be assessed for changes in injury-induced calcium influx. In our study, we showed that preventing injury-induced membrane depolarization via temporal expression of KCNJ2 was sufficient to significantly impair dendrite regeneration, suggesting that depolarization-induced calcium influx promotes dendrite regeneration.

### 3.4. Early-stage signaling with late-stage regenerative consequences

We have identified L-type VGCCs, $IP_3$ signaling, and protein kinase D activity as molecular mediators of dendrite regeneration. L-type VGCCs have long been appreciated for their

roles in neurite outgrowth (Kulbatski et al., 2004; Robson and Burgoyne, 1989) and have been shown to be essential mediators of dendritic development (Tao et al., 2022; Konur and Ghosh, 2005), axonal repair (Ghosh-Roy et al., 2010), and stimulus-evoked sensory processing (Suzuki et al., 2003). A handful of studies, however, have provided evidence that the pore-forming subunits of L-type VGCCs are inhibitory to peripheral nerve regeneration of DRG neurons and that accessory subunits (α2δ) of these channels are inhibitory to axon regeneration in the CNS, albeit via N and P/Q-type channels (Enes et al., 2010; Tedeschi et al., 2016). These conclusions suggest differential roles for VGCCs across different neuron types within the context of neurite repair, and more careful dissection of their necessity for dendrite injury-induced calcium influx and repair is warranted.

Relocalization of the ER and ER-resident $IP_3Rs$ to regenerating neurite tips is not evident after dendrite injury in class I da neurons, but there did seem to be a global increase in the smooth ER marker across the dendrite arbor after single-branch dendrite injury (Rao et al., 2016). Additionally, $IP_3Rs$ and ryanodine receptors have recently been implicated in stimulus-evoked calcium transients after noxious cold in class III da neurons (Patel et al., 2022). Our results confirm that $IP_3$ signaling does play a role in dendrite regeneration. Future studies may quantify whether global increases in the smooth ER marker are indeed observed after dendrite injury, particularly because dendrite regeneration does not proceed along a uniformly growing neurite as does axon regeneration. In the case of dendrites, concentration of cellular materials at a growing tip may not be the most effective means of regenerating lost dendrites.

Protein kinase D has developmental consequences for dendrite arbors (Czöndör et al., 2009; Yin et al., 2008; Bisbal et al., 2008) and regenerative consequences for axonal repair (Cho et al., 2013). In our neurons, we did not observe any developmental differences in branch number after expression dominant-negative, wild-type, or constitutively active forms of PKD. While we did not observe any evidence of injury-induced nuclear accumulation of PKD in our neurons, we occasionally saw evidence of puncta accumulation in the somatic or dendritic compartments after dendrite injury. Critically, we were able to show that dendrite regeneration is sensitive to normal PKD function as evidence by lower regenerative branch growth in neurons expressing a dominant-negative PKD transgene. A RhoA pathway has been implicated in dendritic Golgi outpost formation of cultured hippocampal neurons, with PKD playing a curical role in controlling tubule fission by inactivating slingshot and cofilin (Quassollo et al., 2015). Golgi outposts shape dendritic morphology, but how exactly this is achieved is a subject of debate as some groups claim Golgi outposts serve as sites of acentrosomal microtubule nucleation while others have generated evidence against this and instead suggest that $\gamma$-tubulin serves this function (Ori-McKenney et al., 2012; Zhou et al., 2014; Nguyen et al., 2014). As a counter to RhoA's potential to induce a pro-regenerative response, studies in motor neurons of the mammalian spinal cord after brachial plexus nerve injury revealed that cell type-specific knockout of RhoA prevented degeneration and supported regeneration of dendritic arbors (Li et al., 2023), providing a clue to the molecular mechanisms underlying dendritic arbor stabilization after axon injury. In all, we posit that dendrite regeneration after dendrite injury is likely sensitive to RhoA signaling, but how this mechanistically intersects with PKD, Golgi outpost formation, and $\gamma$-tubulin-mediated nucleation remains to be discovered.

While our study revealed new fundamental insights into how neurons use calcium to sense dendrite injury and initiate a regenerative response, there are many other cellular processes affected by calcium such as gene expression (Puri, 2020), autophagy (Sukumaran et al., 2021), stress responses (Carreras-Sureda et al., 2018), and mitochondrial energetics (Giorgi et al., 2018). Assessing how these processes are affected by dendrite injury-induced calcium influx will greatly enhance our understanding of dendrite regeneration.

Given the well-established differences in the regenerative potential of axons between neurons in a PNS versus CNS environment, it would be interesting to determine whether dendrite injury detection occurs differently in a CNS environment. While mammalian sensory endings have different structures than the dendrites of the da neurons of Drosophila, mammalian neurons in the CNS have similar elaborate morphologies. One recent study using zebrafish motor neurons established that post-synaptic dendrites could regenerate and that dendrite regeneration proceeds in vertebrate systems (Stone et al., 2022), together suggesting that dendrite regeneration is possible for central neurons. We have yet to determine whether dendrites with dendritic spines detect injury differently. Additionally, aged dendrites might detect injury differently. Our evidence here demonstrates that dendrite injury detection mechanisms are largely conserved across PNS neurons. Dissecting how downstream cellular processes are affected by dendrite injury-induced calcium influx and how they contribute to dendrite repair will be foundational to our understanding of neuronal dendrite regeneration.

## 4. Materials and methods

### 4.1. Drosophila strains

We used the following Drosophila strains: $w^{1118}$;; UAS GCaMP7f (BDSC #80906), $w^{1118}$; UAS-GCaMP7f (BDSC #79031), w*; betaTub60D$^{Pin-1}$/CyO; 2.21-Gal4 (BDSC #26259), w*;; ppk-Gal4 (BDSC #32079), w*;; UAS-KCNJ2.GFP (BDSC #6595), $w^{1118}$; ppk-CD4-tdGFP (BDSC #35842) $y^1$, w*; UAS-KCNJ2.HA (BDSC #92026), w*; tub-Gal80$^{ts}$/TM2 (BDSC #7017), $y^1$, w*; UAS-PKD.GFP (BDSC #94614), $y^1$, w*; UAS-PKD.KD.GFP (BDSC #94615), $y^1$, w*; UAS-PKD.SE.GFP (BDSC #94616). UAS-$IP_3$-sponge.m49 was provided by Dr. Andrew Frank (University of Iowa) and originally generated by Dr. Daisuke Yamamoto (Usui-Aoki et al., 2005).

### 4.2. Two-photon laser injury and imaging – Calcium imaging assay

*Drosophila* embryos were collected on grape plates with yeast paste for four hours to synchronize the age of the animals. After 72 h after egg laying (AEL), larvae were individually immobilized on agarose pads sandwiched between a slide and a coverslip using glycerol as the mounting media. Dendrites or axons were imaged and severed from da neurons using a MaiTai two-photon 900 nm laser mounted on a Zeiss 780/980 LSM microscope using ZEN Black/Blue's bleaching and regions functions. A bleaching power of ~780 mW was used on a 10×10 ROI focused on either a dendrite or an axon. Bleaching window settings were as follows: start bleaching after 30 scans, 20 iterations, different scan speed of 5 (pixel dwell time 12.61$\mu$sec), safe bleach for GaAsP on, 900 nm laser at 65 %. Neurons were imaged for ~3 minutes at 0.242fps (740 frames), and injuries

occurred approximately 7.25 seconds into the imaging session (frame 30). For each animal, one to two neuron(s) from abdominal segments 2–5 were injured and imaged before the animal was subsequently returned to individual housing. At 24 or 72 hours after injury, animals were re-mounted, and neurons were re-imaged to confirm neuronal survival and full neurite severing. Only neurons with obvious survival and neurite severing were included in subsequent analyses and presented data.

### 4.3. Two-photon laser injury and imaging – Regeneration assays

*Drosophila* embryos were collected and mounted as above. Dendrites were severed from da neurons by focusing a MaiTai two-photon 900 nm laser mounted on an Zeiss 780 LSM (Li et al., 2018). For experiments in class I neurons, for distal primary branch injuries, we removed 4–6 dendrite branches mostly from the comb dendrite of ddaE; for proximal injuries, we injured the first dendrite branch point of either the comb or lateral dendrite branch; for terminal injuries, a distal terminal branch located on the comb dendrite was injured. For experiments in class IV neurons, we severed all dendrite branches near the cell body. For both class I and class IV regeneration assays, neurons were re-imaged ~24 h after injury to confirm that the dendrite branches had been severed, and again at 72 h after injury to assess regeneration. Mock-injured control neurons are uninjured neurons from the same larva. For each larva, two neurons from abdominal segments 2–5 were injured and one neuron was used as an uninjured control.

For experiments with $Gal80^{ts}$, embryos were collected as above, immediately placed into an 18°C incubator, and allowed to develop for ~84 h. Egg lay plates were then transferred into a 29.5°C incubator for ~12 h prior to laser injury. After injury at 96 h AEL, animals were individually housed in an 18°C incubator, injury was confirmed 24 h PI, and regeneration was assessed 96 h PI.

### 4.4. Quantification of calcium imaging and regeneration assays

Data were analyzed in ImageJ/Fiji. For the calcium imaging assay, we set 12×12 (class IV neurons) or 10×10 (class I neurons) ROIs (regions of interest) at the soma and a region adjacent to the soma with no detectable GCaMP7f signal as a background. Net fluorescence (F) in the soma ROI was obtained by subtracting background fluorescence at each timepoint. Baseline fluorescence ($F_0$) was obtained by averaging the net fluorescence in the five consecutive frames before neurite injury (i.e., frames 26–30). The change in fluorescence ΔF for each neuron was expressed as the ratio of change with respect to the baseline ($F_t - F_0/F_0$).

For regeneration assays in class I da neurons, Z-stacks of neuronal morphology were converted into MIPs (maximum intensity projections). Dendrite arbors were traced from MIPs using the Simple Neurite Tracer (Longair et al., 2011) plugin in Fiji. For injured neurons, the change in branch number (BN) was expressed as an absolute value normalized to the branch number after injury (BN at 72 h PI – (original BN – severed BN)).For uninjured neurons, the change in BN was expressed as an absolute value with respect to BN at 72 h AEL (BN at 144 h AEL – BN at 72 h AEL).

For regeneration assays in class IV da neurons, raw tile-scan images were converted to Imaris files and tiles were adjusted for animal movement during imaging using Imaris Tile Stitcher. These corrected z-stacks were converted into MIPs in ImageJ and we used the polygon selection tool to select and measure the total area of regenerated dendrites.

### 4.5. Statistical analyses

All statistical analyses were performed in GraphPad Prism. Two-way comparisons were performed using a student's t test with Welch's correction, unless otherwise noted. Experimental designs involving more than two groups were compared using a One-Way Brown-Forsythe and Welch ANOVA test with Dunnett's T3 multiple comparisons test or ordinary one-way ANOVA with Sidak multiple comparisons test. All data are presented as mean ± SEM unless otherwise noted.

Some schematics were created with Biorender.

## Supplementary Material

Refer to Web version on PubMed Central for supplementary material.

## Acknowledgements

The authors would like to acknowledge the following funding sources: NIH grant R00NS097627 (to KTP), NIH grant T32MH119049, the University of California Irvine's (UCI) Undergraduate Research Opportunities Program and Summer Undergraduate Research Program (UROP and SURP), and the University of California's Leadership Excellence through Advanced Degrees (UC LEADs) Program. We thank the UCI Optical Biology Core and Dr. Adeela Syed, PhD for extensive use of the microscopes in their facility. This study was made possible in part through access to the Optical Biology Core Facility of the Developmental Biology Center, a shared resource supported by the Cancer Center Support Grant (CA-62203), the Center for Complex Biological Systems Support Grant (GM-076516), and NIH-S10OD032327 at the University of California, Irvine. The authors would also like to acknowledge Patrick Hwu and Sydney Prange for their intellectual contributions to this work. KTP is a fellow of the Hellman Foundation.

## Data Availability

Data will be made available on request.

## References

Baines RA, Uhler JP, Thompson A, Sweeney ST, Bate M, 2001. Altered electrical properties in DrosophilaNeurons developing without synaptic transmission. J. Neurosci. 21, 1523–1531. [PubMed: 11222642]

Beckers A, Moons L, 2019. Dendritic shrinkage after injury: a cellular killer or a necessity for axonal regeneration? Neural Regen. Res. 14 (8), 1313–1316. [PubMed: 30860164]

Berdan RC, Easaw JC, Wang R, 1993. Alterations in membrane potential after axotomy at different distances from the soma of an identified neuron and the effect of depolarization on neurite outgrowth and calcium channel expression. J. Neurophysiol. 69, 151–164. [PubMed: 8381855]

Bisbal M, et al. , 2008. Protein kinase D regulates trafficking of dendritic membrane proteins in developing neurons. J. Neurosci. 28, 9297–9308. [PubMed: 18784310]

Brown CE, Li P, Boyd JD, Delaney KR, Murphy TH, 2007. Extensive turnover of dendritic spines and vascular remodeling in cortical tissues recovering from stroke. J. Neurosci. 27, 4101–4109. [PubMed: 17428988]

Carreras-Sureda A, Pihán P, Hetz C, 2018. Calcium signaling at the endoplasmic reticulum: fine-tuning stress responses. Cell Calcium 70, 24–31. [PubMed: 29054537]

Chen L, Stone MC, Tao J, Rolls MM, 2012. Axon injury and stress trigger a microtubule-based neuroprotective pathway. Proc. Natl. Acad. Sci. 109, 11842–11847. [PubMed: 22733771]

Cho Y, Cavalli V, 2012. HDAC5 is a novel injury-regulated tubulin deacetylase controlling axon regeneration. EMBO J 31 (14), 3063–3078. [PubMed: 22692128]

Cho Y, Sloutsky R, Naegle KM, Cavalli V, 2013. Injury-Induced HDAC5 Nuclear Export Is Essential for Axon Regeneration. Cell 155, 894–908. [PubMed: 24209626]

Cohan CS, Kater SB, 1986. Suppression of neurite elongation and growth cone motility by electrical activity. Science 232, 1638–1640. [PubMed: 3715470]

Czöndör K, et al. , 2009. Protein kinase D controls the integrity of golgi apparatus and the maintenance of dendritic arborization in hippocampal neurons. Mol. Biol. Cell 20, 2108–2120. [PubMed: 19211839]

Dana H, et al. , 2019. High-performance calcium sensors for imaging activity in neuronal populations and microcompartments. Nat. Methods 16, 649–657. [PubMed: 31209382]

DeVault L, et al. , 2018. Dendrite regeneration of adult Drosophila sensory neurons diminishes with aging and is inhibited by epidermal-derived matrix metalloproteinase 2. Genes Dev. 32, 402–414. [PubMed: 29563183]

Ding C, Hammarlund M, 2019. Mechanisms of injury-induced axon degeneration. Curr. Opin. Neurobiol. 57, 171–178. [PubMed: 31071521]

ElAbd R, et al. , 2022. Role of electrical stimulation in peripheral nerve regeneration: a systematic review. Plast. Reconstr. Surg. – Glob. Open 10, e4115. [PubMed: 35317464]

Enes J, et al. , 2010. Electrical activity suppresses axon growth through Cav1.2 channels in adult primary sensory neurons. Curr. Biol. 20, 1154–1164. [PubMed: 20579880]

Fitzpatrick JS, et al. , 2009. Inositol-1,4,5-trisphosphate receptor-mediated Ca2+ waves in pyramidal neuron dendrites propagate through hot spots and cold spots. J. Physiol. 587, 1439–1459. [PubMed: 19204047]

Furusawa K, Emoto K, 2021. Scrap and build for functional neural circuits: spatiotemporal regulation of dendrite degeneration and regeneration in neural development and disease. Front. Cell. Neurosci. 14.

Ghosh-Roy A, Wu Z, Goncharov A, Jin Y, Chisholm AD, 2010. Calcium and cyclic AMP promote axonal regeneration in caenorhabditis elegans and require DLK-1 Kinase. J. Neurosci. 30, 3175–3183. [PubMed: 20203177]

Giorgi C, Marchi S, Pinton P, 2018. The machineries, regulation and cellular functions of mitochondrial calcium. Nat. Rev. Mol. Cell Biol. 19, 713–730. [PubMed: 30143745]

Gordon T, 2016. Electrical stimulation to enhance axon regeneration after peripheral nerve injuries in animal models and humans. Neurotherapeutics 13, 295–310. [PubMed: 26754579]

Grueber WB, Jan LY, Jan YN, 2002. Tiling of the Drosophila epidermis by multidendritic sensory neurons. Development 129, 2867–2878. [PubMed: 12050135]

Hammarlund M, Nix P, Hauth L, Jorgensen EM, Bastiani M, 2009. Axon regeneration requires a conserved MAP kinase pathway. Science 323, 802–806. [PubMed: 19164707]

Hao Y, Collins C, 2017. Intrinsic mechanisms for axon regeneration: insights from injured axons in Drosophila. Curr. Opin. Genet. Dev. 44, 84–91. [PubMed: 28232273]

Hertzler JI, et al. , 2020. Kinetochore proteins suppress neuronal microtubule dynamics and promote dendrite regeneration. Mol. Biol. Cell 31, 2125–2138. [PubMed: 32673176]

Hughes CL, Thomas JB, 2007. A sensory feedback circuit coordinates muscle activity in Drosophila. Molecular and Cellular Neuroscience 35 (2), 383–396. [PubMed: 17498969]

Jara JS, Agger S, Hollis ER, 2020. Functional electrical stimulation and the modulation of the axon regeneration program. Front. Cell Dev. Biol. 8.

Javeed S, Faraji AH, Dy C, Ray WZ, MacEwan MR, 2021. Application of electrical stimulation for peripheral nerve regeneration: stimulation parameters and future horizons. Interdiscip. Neurosurg. 24, 101117.

Kamber D, Erez H, Spira ME, 2009. Local calcium-dependent mechanisms determine whether a cut axonal end assembles a retarded endbulb or competent growth cone. Exp. Neurol. 219, 112–125. [PubMed: 19442660]

Kiernan MC, et al. , 2011. Amyotrophic lateral sclerosis. Lancet 377, 942–955. [PubMed: 21296405]

Konur S, Ghosh A, 2005. Calcium signaling and the control of dendritic development. Neuron 46, 401–405. [PubMed: 15882639]

Kulbatski I, Cook DJ, Tator CH, 2004. Calcium entry through L-type calcium channels is essential for neurite regeneration in cultured sympathetic neurons. J. Neurotrauma 21, 357–374. [PubMed: 15115609]

Li S, et al. , 2016. Promoting axon regeneration in the adult CNS by modulation of the melanopsin/GPCR signaling. Proc. Natl. Acad. Sci. 113, 1937–1942. [PubMed: 26831088]

Li M, et al. , 2023. Motor neuron-specific RhoA knockout delays degeneration and promotes regeneration of dendrites in spinal ventral horn after brachial plexus injury. Neural Regen. Res. 18, 2757. [PubMed: 37449641]

Li D, Li F, Guttipatti P, Song Y, 2018. A drosophila in vivo injury Model for studying neuroregeneration in the peripheral and central nervous system. J. Vis. Exp. 135, e57557.

Longair MH, Baker DA, Armstrong JD, 2011. Simple Neurite Tracer: open source software for reconstruction, visualization and analysis of neuronal processes. Bioinformatics 27, 2453–2454. [PubMed: 21727141]

Mahar M, Cavalli V, 2018. Intrinsic mechanisms of neuronal axon regeneration. Nat. Rev. Neurosci. 19, 323–337. [PubMed: 29666508]

Maier D, et al. , 2006. Drosophila protein kinase D is broadly expressed and a fraction localizes to the Golgi compartment. Gene Expr. Patterns 6, 849–856. [PubMed: 16750940]

Mandolesi G, Madeddu F, Bozzi Y, Maffei L, Ratto GM, 2004. Acute physiological response of mammalian central neurons to axotomy: ionic regulation and electrical activity. FASEB J. 18, 1934–1936. [PubMed: 15451889]

Mauceri D, et al. , 2020. Nasally delivered VEGFD mimetics mitigate stroke-induced dendrite loss and brain damage. Proc. Natl. Acad. Sci. U. S. A. 117, 8616–8623. [PubMed: 32229571]

McGuire SE, Le PT, Osborn AJ, Matsumoto K, Davis RL, 2003. Spatiotemporal Rescue of Memory Dysfunction in Drosophila. Science 302 (5651), 1765–1768. [PubMed: 14657498]

Nguyen MM, et al. , 2014. γ-Tubulin controls neuronal microtubule polarity independently of Golgi outposts. Mol. Biol. Cell 25, 2039–2050. [PubMed: 24807906]

Ori-McKenney KM, Jan LY, Jan Y-N, 2012. Golgi outposts shape dendrite morphology by functioning as sites of acentrosomal microtubule nucleation in neurons. Neuron 76, 921–930. [PubMed: 23217741]

Park KK, et al. , 2008. Promoting axon regeneration in the adult CNS by modulation of the PTEN/mTOR pathway. Science 322, 963–966. [PubMed: 18988856]

Parrish JZ, Xu P, Kim CC, Jan LY, Jan YN, 2009. The microRNA bantam functions in epithelial cells to regulate scaling growth of dendrite arbors in Drosophila neurons. Neuron 63, 788–802. [PubMed: 19778508]

Patel AA, Sakurai A, Himmel NJ, Cox DN, 2022. Modality specific roles for metabotropic GABAergic signaling and calcium induced calcium release mechanisms in regulating cold nociception. Front. Mol. Neurosci. 15.

Puri BK, 2020. Calcium Signaling and Gene Expression. In: Islam Md., S.) (Ed.), Calcium Signaling. Springer International Publishing, Cham, pp. 537–545. 10.1007/978-3-030-12457-1_22.

Quassollo G, et al. , 2015. A RhoA signaling pathway regulates dendritic Golgi outpost formation. Curr. Biol. 25, 971–982. [PubMed: 25802147]

Rao K, et al. , 2016. Spastin, atlastin, and ER relocalization are involved in axon but not dendrite regeneration. Mol. Biol. Cell 27, 3245–3256. [PubMed: 27605706]

Rao KS, Rolls MM, 2017. Two Drosophila model neurons can regenerate axons from the stump or from a converted dendrite, with feedback between the two sites. Neural Dev. 12, 15. [PubMed: 28818097]

Reddish FN, et al. , 2021. Rapid subcellular calcium responses and dynamics by calcium sensor G-CatchER+. iScience 24, 102129. [PubMed: 33665552]

Rishal I, Fainzilber M, 2014. Axon–soma communication in neuronal injury. Nat. Rev. Neurosci. 15, 32–42. [PubMed: 24326686]

Robson SJ, Burgoyne RD, 1989. L-type calcium channels in the regulation of neurite outgrowth from rat dorsal root ganglion neurons in culture. Neurosci. Lett. 104, 110–114. [PubMed: 2554216]

Rolls MM, et al. , 2007. Polarity and intracellular compartmentalization of Drosophila neurons. Neural Dev. 2, 7. [PubMed: 17470283]

Shin JE, et al. , 2012. Dual Leucine Zipper Kinase Is Required for Retrograde Injury Signaling and Axonal Regeneration. Neuron 74, 1015–1022. [PubMed: 22726832]

Song Y, et al. , 2012. Regeneration of Drosophila sensory neuron axons and dendrites is regulated by the Akt pathway involving Pten and microRNA bantam. Genes Dev. 26, 1612–1625. [PubMed: 22759636]

Stone MC, Albertson RM, Chen L, Rolls MM, 2014. Dendrite injury triggers DLK-independent regeneration. Cell Rep. 6, 247–253. [PubMed: 24412365]

Stone MC, Nguyen MM, Tao J, Allender DL, Rolls MM, 2010. Global up-regulation of microtubule dynamics and polarity reversal during regeneration of an axon from a dendrite. Mol. Biol. Cell 21, 767–777. [PubMed: 20053676]

Stone MC, Roegiers F, Rolls MM, 2008. Microtubules have opposite orientation in axons and dendrites of drosophila neurons. Mol. Biol. Cell 19, 4122–4129. [PubMed: 18667536]

Stone MC, Seebold DY, Shorey M, Kothe GO, Rolls MM, 2022. Dendrite regeneration in the vertebrate spinal cord. Dev. Biol. 488, 114–119. [PubMed: 35644253]

Strautman AF, Cork RJ, Robinson KR, 1990. The distribution of free calcium in transected spinal axons and its modulation by applied electrical fields. J. Neurosci. 10, 3564–3575. [PubMed: 2230946]

Sukumaran P, et al. , 2021. Calcium signaling regulates autophagy and apoptosis. Cells 10, 2125. [PubMed: 34440894]

Sun L, et al. , 2014. Neuronal regeneration in C. elegans requires subcellular calcium release by ryanodine receptor channels and can be enhanced by optogenetic stimulation. J. Neurosci. 34, 15947–15956. [PubMed: 25429136]

Suzuki H, et al. , 2003. In Vivo Imaging of *C. elegans* mechanosensory neurons demonstrates a specific role for the MEC-4 channel in the process of gentle touch sensation. Neuron 39, 1005–1017. [PubMed: 12971899]

Tao L, Coakley S, Shi R, Shen K, 2022. Dendrites use mechanosensitive channels to proofread ligand-mediated neurite extension during morphogenesis. Dev. Cell 57, 1615–1629.e3. [PubMed: 35709764]

Tedeschi A, et al. , 2016. The calcium channel subunit Alpha2delta2 suppresses axon regeneration in the adult CNS. Neuron 92, 419–434. [PubMed: 27720483]

Thompson-Peer KL, DeVault L, Li T, Jan LY, Jan YN, 2016. In vivo dendrite regeneration after injury is different from dendrite development. Genes Dev. 30, 1776–1789. [PubMed: 27542831]

Tuszynski MH, Steward O, 2012. Concepts and Methods for the Study of Axonal Regeneration in the CNS. Neuron 74 (5), 777–791. [PubMed: 22681683]

Usui-Aoki K, et al. , 2005. Targeted expression of Ip3 Sponge and Ip3 Dsrna impaires sugar taste sensation in drosophila. J. Neurogenet. 19, 123–141. [PubMed: 16540404]

Valakh V, Frey E, Babetto E, Walker LJ, DiAntonio A, 2015. Cytoskeletal disruption activates the DLK/JNK pathway, which promotes axonal regeneration and mimics a preconditioning injury. Neurobiol. Dis. 77, 13–25. [PubMed: 25726747]

Wang F, et al. , 2023. Gliotransmission and adenosine signaling promote axon regeneration. Dev. Cell 58, 660–676.e7. [PubMed: 37028426]

Wolf JA, Stys PK, Lusardi T, Meaney D, Smith DH, 2001. Traumatic axonal injury induces calcium influx modulated by tetrodotoxin-sensitive sodium channels. J. Neurosci. 21, 1923–1930. [PubMed: 11245677]

Xiang Y, et al. , 2010. Light-avoidance-mediating photoreceptors tile the Drosophila larval body wall. Nature 468, 921–926. [PubMed: 21068723]

Xiong X, et al. , 2010. Protein turnover of the Wallenda/DLK kinase regulates a retrograde response to axonal injury. J. Cell Biol. 191, 211–223. [PubMed: 20921142]

Xiong Y, Mahmood A, Chopp M, 2019. Remodeling dendritic spines for treatment of traumatic brain injury. Neural Regen. Res. 14, 1477. [PubMed: 31089035]

Yan D, Wu Z, Chisholm AD, Jin Y, 2009. The DLK-1 Kinase Promotes mRNA Stability and Local Translation in C. elegans Synapses and Axon Regeneration. Cell 138, 1005–1018. [PubMed: 19737525]

Yang Y, et al. , 2018. Improved calcium sensor GCaMP-X overcomes the calcium channel perturbations induced by the calmodulin in GCaMP. Nat. Commun. 9, 1504. [PubMed: 29666364]

Yin D-M, Huang Y-H, Zhu Y-B, Wang Y, 2008. Both the establishment and maintenance of neuronal polarity require the activity of protein Kinase D in the Golgi apparatus. J. Neurosci. 28, 8832–8843. [PubMed: 18753385]

Zhou W, et al. , 2014. GM130 Is Required for compartmental organization of dendritic Golgi outposts. Curr. Biol. 24, 1227–1233. [PubMed: 24835455]

Ziv NE, Spira ME, 1993. Spatiotemporal Distribution of Ca2+ following axotomy and throughout the recovery process of cultured aplysia neurons. Eur. J. Neurosci. 5, 657–668. [PubMed: 8261139]

Ziv NE, Spira ME, 1995. Axotomy induces a transient and localized elevation of the free intracellular calcium concentration to the millimolar range. J. Neurophysiol. 74, 2625–2637. [PubMed: 8747220]

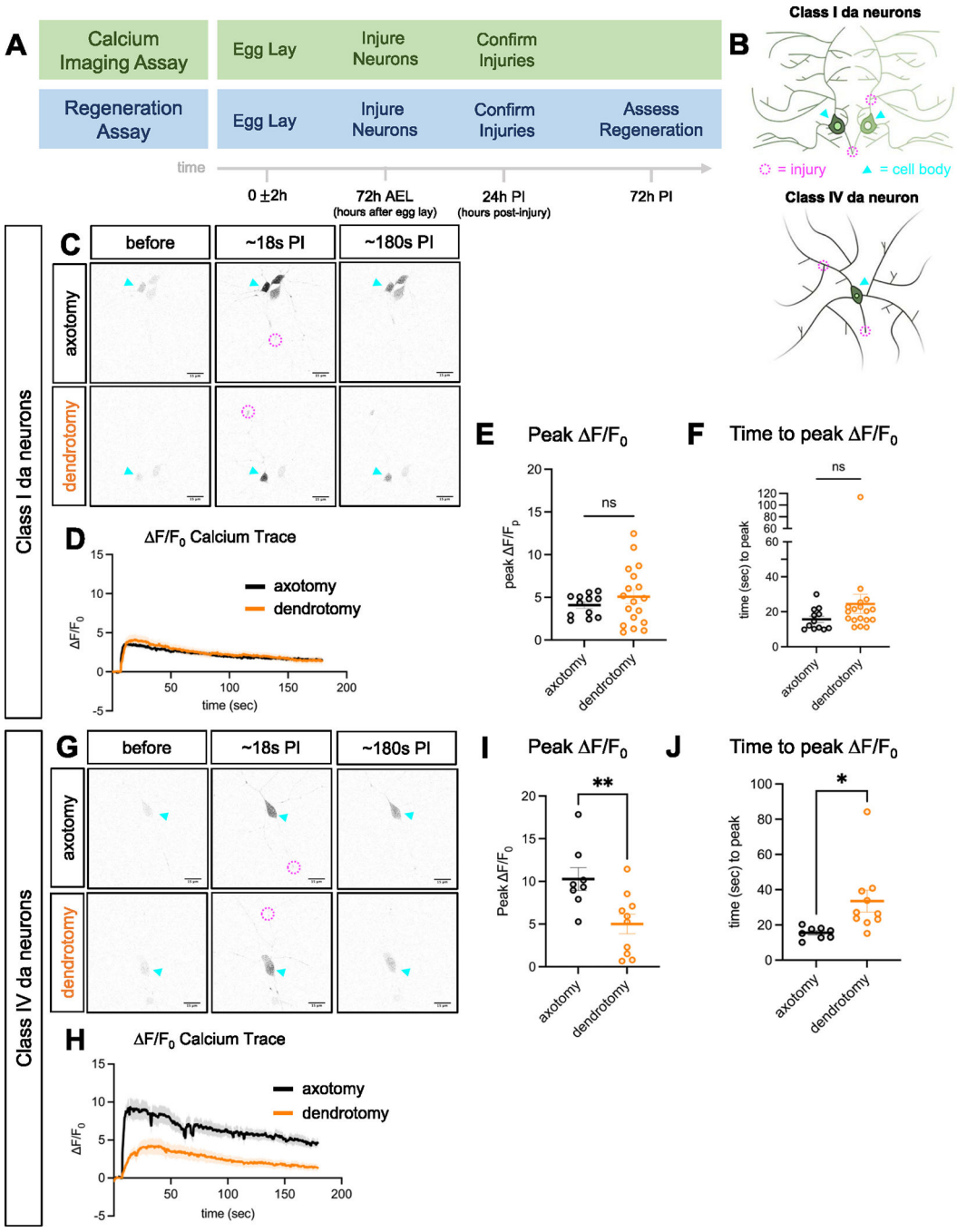


**Fig. 1. Dendrite injury triggers rapid somatic calcium influx.**

**(A)** Timeline of experimental assays used throughout the study. **(B)** BioRender-generated graphics of neuron types used in this study. Throughout the figures, magenta dashed circles indicate the site of injury and cyan arrowheads indicate cell bodies. **(C, G)** Representative images of class I ddaE or class IV ddaC neurons before, 18 s after, and 180 s after injury. Scale bar, 15$\mu$m. **(D,H)** $\Delta F/F_0$ Calcium traces after axotomy (black) or dendrotomy (orange) of class I ddaE or class IV ddaC neurons. **(E, F, I, J)** Quantifications of peak $\Delta F/F_0$ and time

(sec) to peak $\Delta F/F_0$. Values are plotted as mean ± SEM. **p < 0.01. *p < 0.05 by unpaired **(I)** or Welch's **(E, F, J)** t-test.

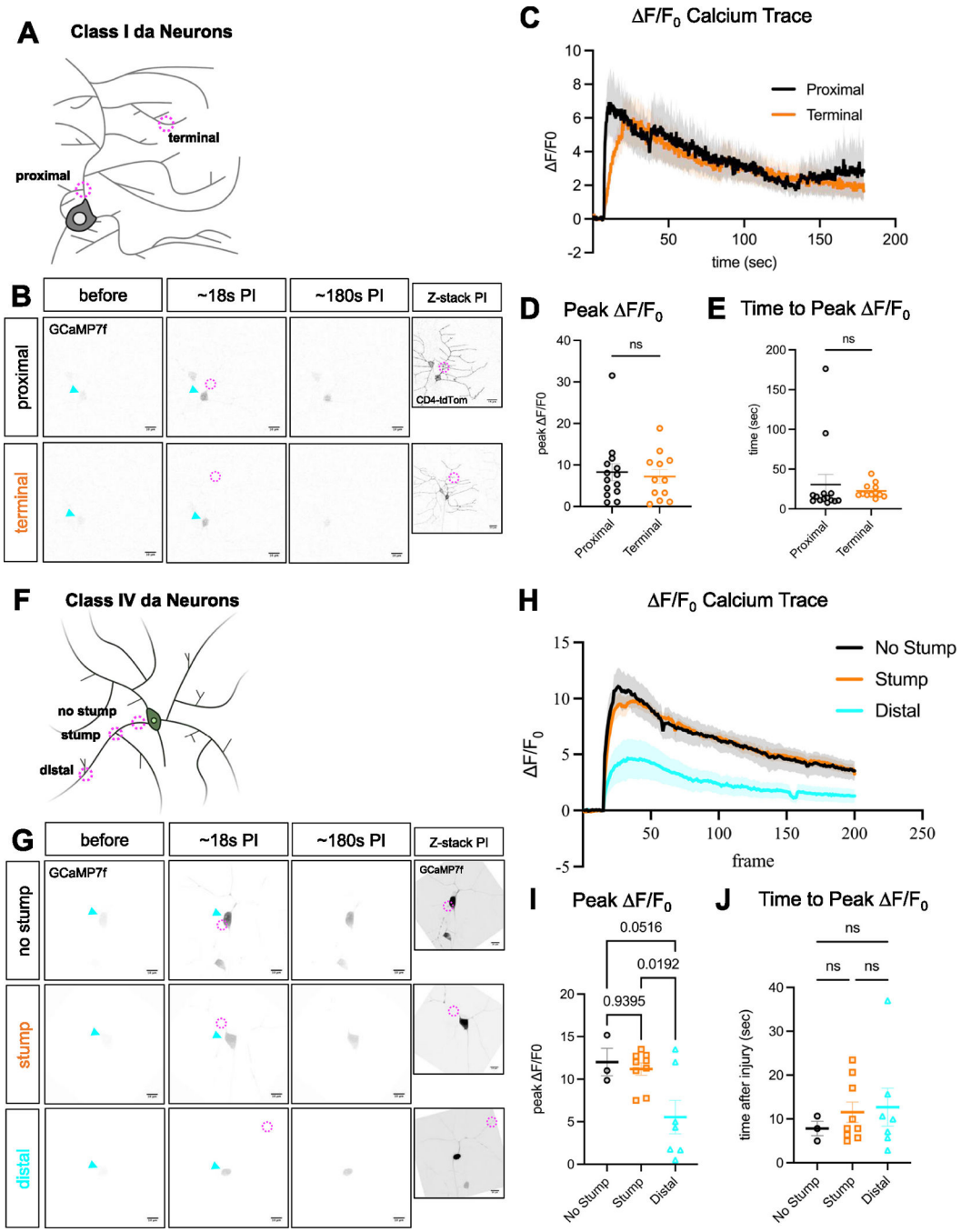


**Fig. 2. Injury-induced calcium influx is sensitive to distance in class IV but not class I neurons.**

**(A, F)** Graphics depicting different sites of injury to class I ddaE and class IV ddaC dendrite arbors. **(B)** Representative images of the GCaMP7f signal in class I ddaE neurons before injury, ~18 sec PI, and ~180 s PI. Maximum intensity projections with a membrane-bound tdTomato label are also provided to visualize the injury site more clearly. Scale Bar = 10$\mu$m. **(C)** Somatic $\Delta F/F_0$ plot after proximal and terminal injuries. **(D, E)** Peak and time to peak somatic $\Delta F/F_0$ plots. **(G)** Representative images of the GCaMP7f signal in class IV ddaC neurons before injury, ~18 s PI, and ~180 s PI. Maximum intensity projections with digitally

enhanced GCaMP7f signal provided to visualize the injury site more clearly. **(H)** Somatic $\Delta F/F_0$ plot after no stump, stump, and distal injuries. **(I, J)** Peak and time to peak somatic $\Delta F/F_0$ plots.

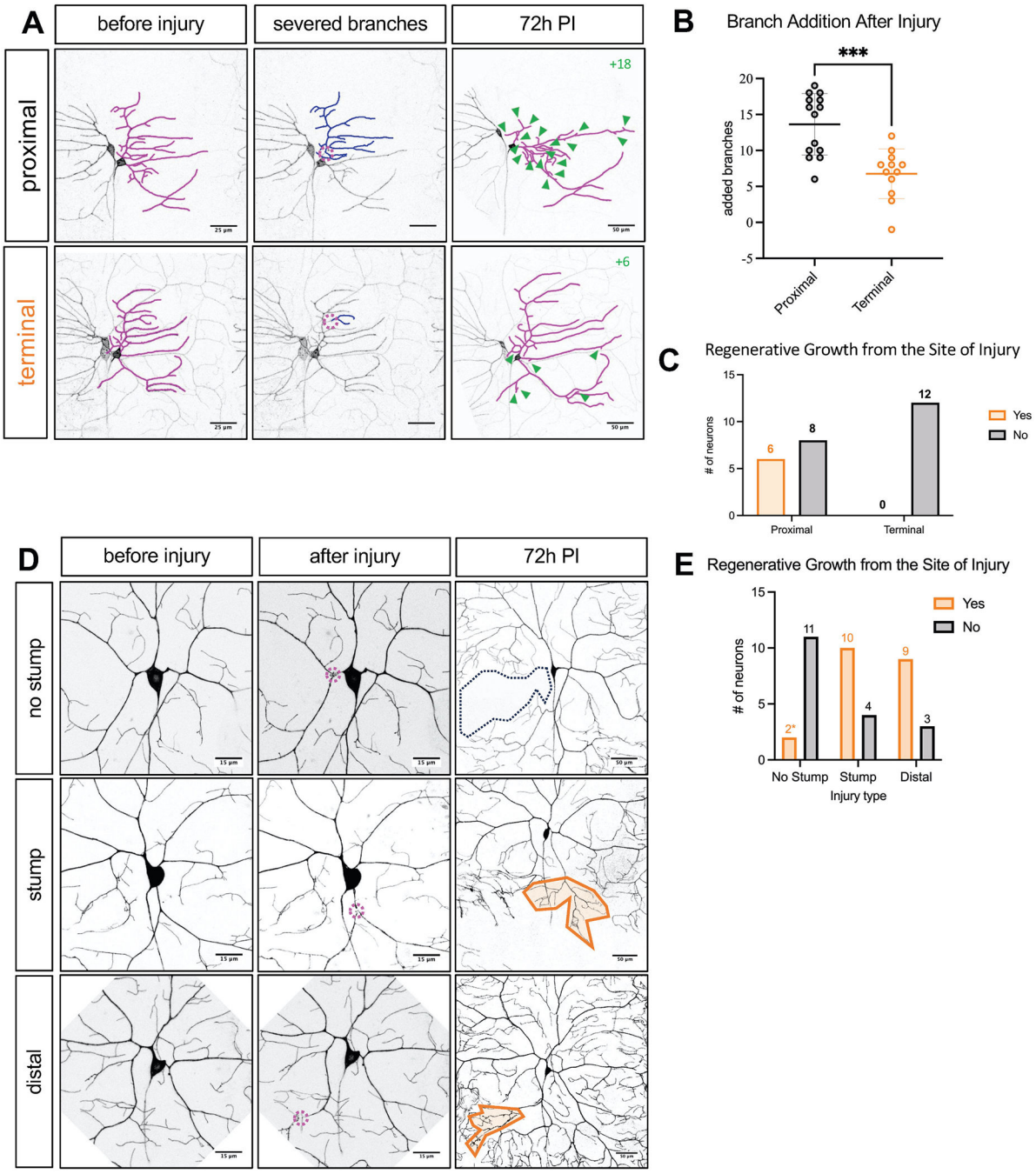


**Fig. 3. Dendrite injury at different sites triggers varying levels of dendrite repair.**

**(A)** Representative images of class I ddaE neurons before proximal or terminal branch injury, after injury with indication of severed branches (blue overlay), and 72 h PI with indications of regenerated branches (green arrowheads and total branches added in upper right). **(B)** Quantified branch addition after injury to either proximal or terminal dendrite branches. **(C)** Number of neurons displaying regenerative growth from the site of injury after injury to either proximal or terminal dendrite branches. **(D)** Representative images of class IV ddaC neurons before injury, after injury, or 72 h PI with indications for areas of

regrowth or lack thereof. **(E)** Number of neurons displaying regenerative growth from the site of injury after no stump, stump, and distal injuries.

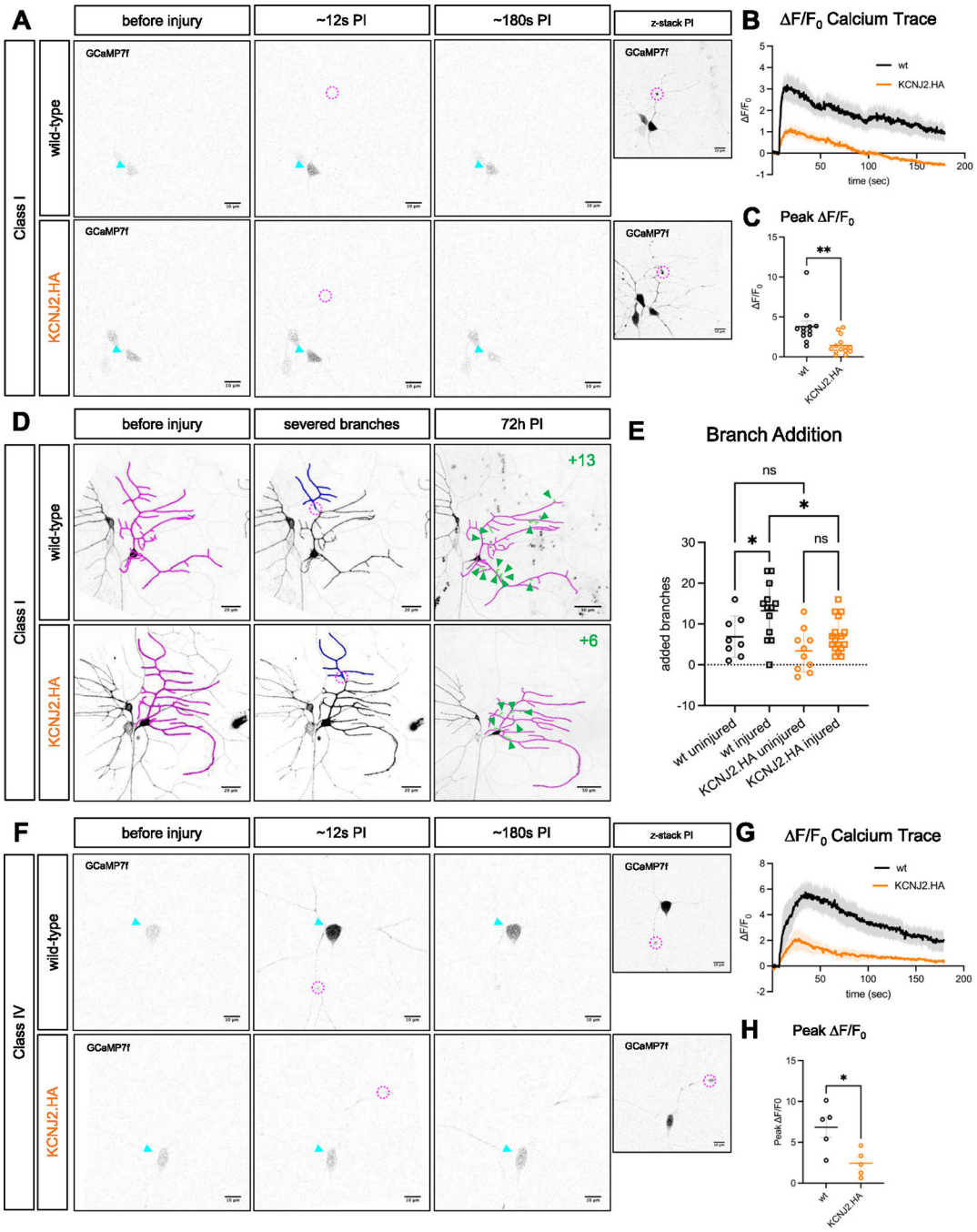


**Fig. 4. KCNJ2-mediated electrical silencing shunts injury-induced calcium influx.**

**(A)** Representative GCaMP7f images of wild-type or KCNJ2.HA-expressing class I ddaE neurons before injury, ~12 s PI, and ~180 s PI. Maximum intensity projections with digitally enhanced GCaMP7f signal provided to visualize the injury site more clearly. Scale bars = 10 $\mu$m. **(B)** Somatic $\Delta F/F_0$ calcium trace of wild-type (black) or KCNJ2.HA-expressing neurons (orange). **(C)** Quantification of peak somatic $\Delta F/F_0$. Values are plotted as mean ± SEM. **p < 0.01 by Welch's t-test. **(D)** Representative images of class I ddaE neurons expressing CD4-tdTomato before injury (magenta = traced dendrite arbor, scale bar =

20$\mu$m), after injury (blue = severed branches, scale bar = 20$\mu$m), and 72 h PI (green arrowheads denote regenerated branches, scale bar = 50$\mu$m). **(E)** Quantified branch addition in uninjured and injured neurons of both genotypes compared using ordinary one-way ANOVA with Sidak multiple comparisons testing. **(F)** Representative GCaMP7f images of wild-type or KCNJ2.HA-expressing class IV ddaC neurons before injury, ~12 s PI, and ~180 s PI. Maximum intensity projections with digitally enhanced GCaMP7f signal provided to visualize the injury site more clearly (scale bars = 10 $\mu$m). **(G)** Somatic $\Delta F/F_0$ calcium trace. **(H)** Quantification of peak somatic $\Delta F/F_0$. Values are plotted as mean ± SEM. *$p < 0.05$ by Welch's t-test.

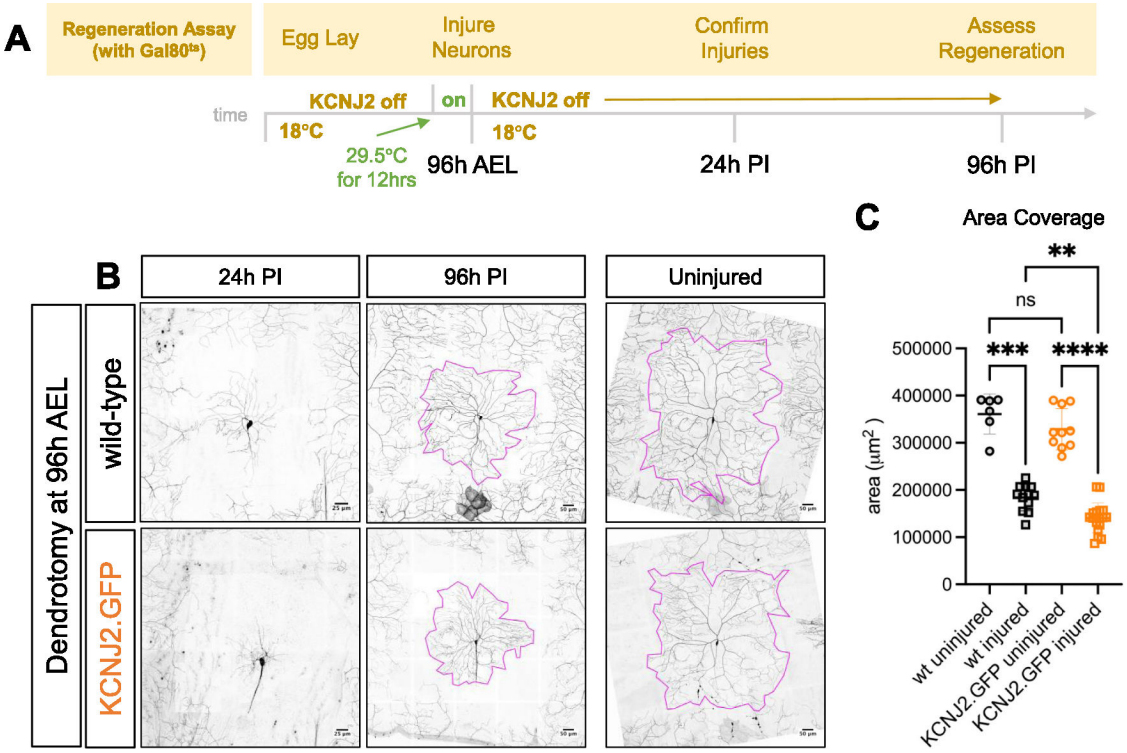


**Fig. 5. KCNJ2 expression only at the time of injury is sufficient to block dendrite regeneration.**

**(A)** Timeline of the regeneration assay with Gal80$^{ts}$. KCNJ2. GFP expression was restricted during development, induced 12 hours prior to injury, and restricted again immediately after injury. **(B)** Representative images of wild-type or KCNJ.GFP-expressing class IV ddaC neurons at 24 h PI (scale bars = 25 $\mu$m), 96 h PI (scale bars = 50$\mu$m), or uninjured controls at 192 h AEL (identical timepoint as 96 h PI; scale bars = 50$\mu$m). **(C)** Quantification of area coverage represented by magenta selection areas in (B). Values are plotted as mean ± SD. ****$p < 0.0001$, ***$p < 0.001$, **$p < 0.01$ by ordinary one-way ANOVA with Sidak multiple comparisons test.

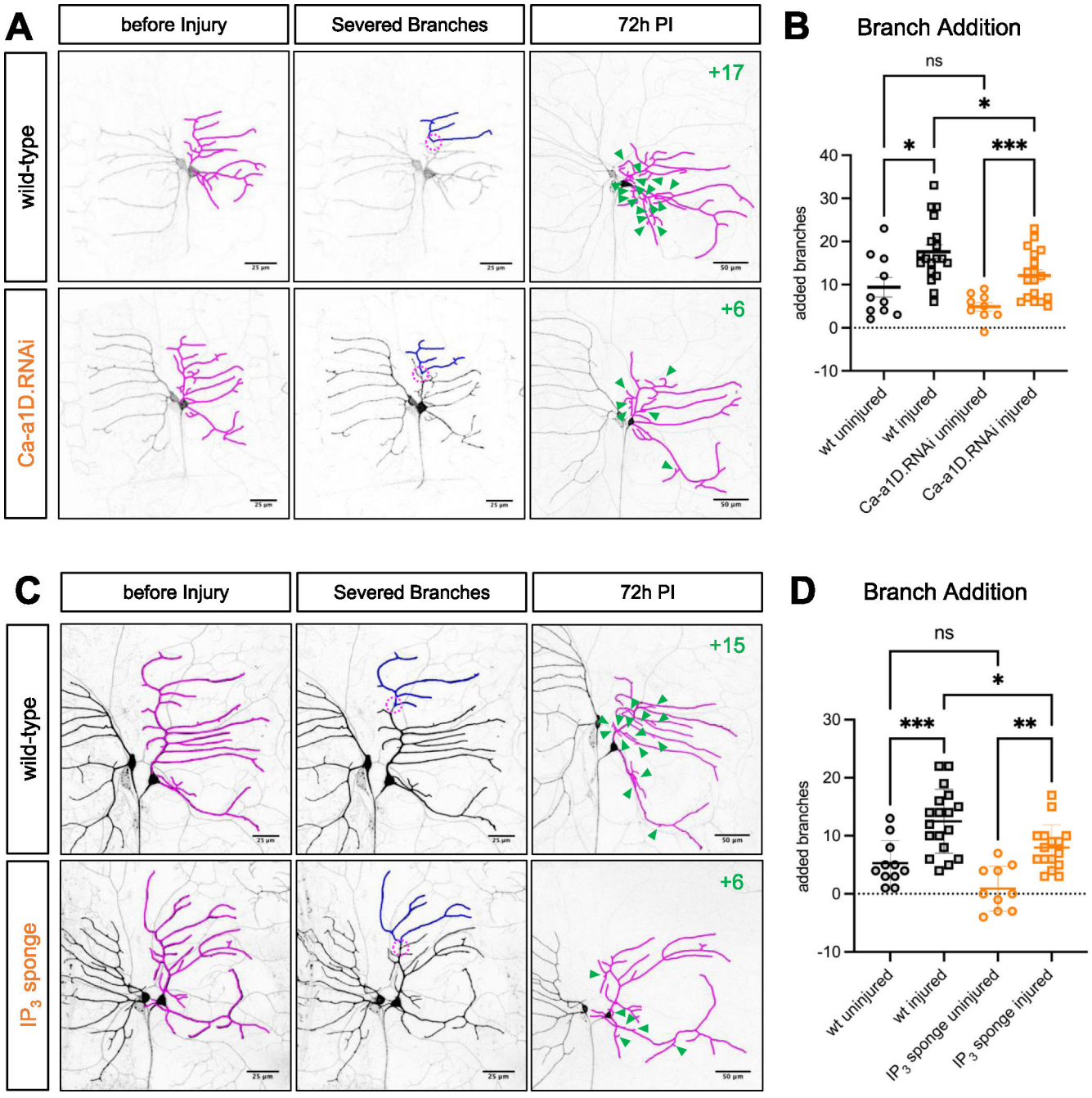


**Fig. 6. Knockdown of L-type VGCCs and inhibition of $IP_3$ signaling impairs dendrite regeneration**

**(A)** Representative images of wild-type or Ca-a1D.RNAi-expressing class I ddaE neurons before injury (magenta = traced arbors; scale bar = 25$\mu$m), after injury (blue = trace of severed branches; scale bar = 25$\mu$m), or 72 h PI (magenta = traced arbors, green arrowheads = regenerated branches; scale bar = 50 $\mu$m). **(B)** Quantification of added branches in uninjured and injured neurons. **(C)** Representative images of wild-type or $IP_3$-sponge expressing class I ddaE neurons as in (A). **(D)** Quantification of added branches as in

(B). Values are plotted as mean ± SEM. ***p < 0.001, **p < 0.01, *p < 0.05 by ordinary one-way ANOVA with Sidak multiple comparisons test.

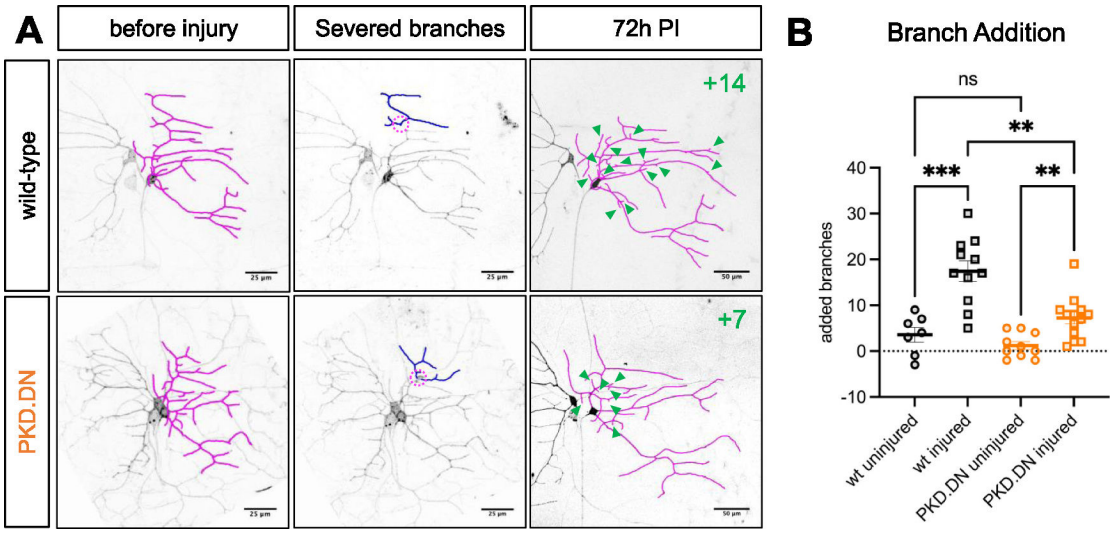


**Fig. 7. Protein kinase D activity regulates dendrite regeneration.**

**(A)** Representative images of wild-type or PKD.DN-expressing class I ddaE neurons before injury (magenta = traced dendrite arbor, scale bars = 25$\mu$m), after injury (blue = severed dendrite branches, scale bars = 25$\mu$m), or 72 h PI (green arrowheads = regenerated branches, scale bars = 50$\mu$m). **(B)** Quantification of added branches at 72 h PI for uninjured and injured neurons. Values are plotted as mean ± SEM. ***p < 0.001, **p < 0.01 by ordinary one-way ANOVA with Sidak multiple comparisons test.